Journal of Natural Gas Science and Engineering 26 (2015) 6–17

Contents lists available at ScienceDirect

Journal of Natural Gas Science and Engineering

journal homepage: www.elsevier.com/locate/jngse

Optimizing natural gas reciprocating expansion engines for Town Border pressure reduction stations based on AGA8 equation of state

M. Farzaneh-Gord [a], S. Izadi [b], M. Deymi-Dashtebayaz [c, *], Seyed Iman Pishbin [d], Hamideh Sheikhani [e]

[a] The Faculty of Mechanical Engineering, Shahrood University of Technology, Shahrood, Iran
[b] Master Student of Mechanical Engineering, Shahrood University of Technology, Shahrood, Iran
[c] The Faculty of Mechanical Engineering, Hakim Sabzevari University, Sabzevar, Iran
[d] The Faculty of Mechanical Engineering, Khayym University of Mashhad, Mashhad, Iran
[e] Industrial Advisor of Khorasanrazavi Gas Company, Mashhad, Iran

ARTICLE INFO

Article history:
Received 9 December 2014
Received in revised form
21 May 2015
Accepted 23 May 2015
Available online xxx

Keywords:
Expansion engine
Thermodynamic analysis
Optimization
AGA8 equation

ABSTRACT

In the supply pipelines, the natural gas pressure is about 1.7 MPa (approximately 250 Psi) and before entering distribution pipelines, this pressure should be reduced to a lower level of 0.4 MPa (approximately 60Psi). This press ure reduction is performed in Town Border Stations (TBSs) in which the sizeable amount of pressure energy is wasted by employing throttling valves. One way to recover pressure energy during pressure reduction process is to employ an expansion machine such as the reciprocating expansion engines. The purpose of this study is thermodynamic simulation of one-sided medium pressure reciprocating expansion engine. The simulation is based on energy and mass conservation laws and the AGA8 equation of state. The results show that, with using expansion engine in TBS stations the efficiency of pressure energy recovery is about 91%. Also, with the suction of 18 g gas per cycle, the engine generates 46.2 kW power. The results also show that the engine could generate highest power at specific suction port to bore diameter.

1. Introduction

Environment protection and energy conservation have led researchers to keep looking for effective ways of energy management. Natural gas pipelines are one of the sections which waste a lot of energy during gas conveyance. In various countries (including Iran), the pressure of natural gas in supply pipelines is about 1.7 MPa (approximately 250 Psi). At consumption points, the pressure of the gas must be reduced. This pressure reduction takes place in Town Border Stations (TBSs). At TBSs, the pressure is reduced from 1.7 MPa (approximately 250 Psi) to 0.4 MPa (approximately 60 Psi) by employing throttling valves, which waste large amount of pressure energy (availability). Several methods have been proposed for recovering this huge wasted energy (Querol et al., 2011; Farzaneh-Gord and Deymi-Dashtebayaz, 2009; Chaczykowski et al., 2011; He and Ju, 2014; Farzaneh-Gord and Kargaran, 2010; Farzaneh-Gord and Sadi, 2008; Rosen and Scott, 1998).

Many researchers have investigated the use of natural gas pressure energy, focusing on the pressure drop stations. Bisio (Bisio, 1995) is one of the researchers that proposed systems to use this wasted energy, including a mechanical system to compress air. Another method for using natural gas pressure energy is expansion turbines (turbo expanders) that generate electricity (Greeff et al., 2004; Farzaneh-Gord and Deymi-Dashtebayaz, 2008; Farzaneh-Gord and Maghrebi, 2009; Farzaneh-Gord et al., 2009; Kostowski et al., 2014; Kostowski and Usón, 2013). In one study, Greeff et al. (Greeff et al., 2004) have investigated merging of expander turbines into different high-pressure exothermic chemical-synthesis processes. They illustrated prospering integration of an expander turbine with remarkable energy savings. Farzaneh-Gord and Deymi-Dashtebayaz (Farzaneh-Gord and Deymi-Dashtebayaz, 2008) undertook an extensive feasibility study on producing required electricity for Khangiran gas refinery from its pressure reduction station. The conclusion drawn from the results indicated that the amount of available energy could meet all electrical demands of the refinery. Also Kostowski and Usón (Kostowski and Usón, 2013) presented a thermoeconomic assessment of an expansion system applied in the natural gas transportation process. Their system

* Corresponding author.
E-mail address: meh_deimi@yahoo.com (M. Deymi-Dashtebayaz).

http://dx.doi.org/10.1016/j.jngse.2015.05.025
1875-5100/

consists of two turbo expander stages reducing the natural gas pressure and providing mechanical energy to drive electric generators.

In addition to turbo expander for alternative pressure reduction, reciprocating expansion engine is the other method for simultaneous pressure reduction and work generation. There is a limited study on this novel scenario for pressure reduction. Tuma and Sekavcnik (Tuma and Sekavcnik, 1997) depicted enthalpy–entropy diagrams for expansion of various natural gas compositions for employ in electrical power generation via expansion engines. In another study, Farzaneh Gord and Jannatabadi (Farzaneh Gord and Jannatabadi, 2014) simulated the single acting natural gas reciprocating expansion engine based on ideal gas model for using in City Gate Stations (CGSs). In their research various parameters including the inlet port diameter, connecting rod length, crank radius and engine speed have been investigated on performance reciprocating engine.

Due to limited studies on reciprocating expansion engine, it is instructive to review researches on reciprocating compressors as similar machine. Reciprocating compressors are common equipment in industry for producing high pressure compressed gas. These compressors have been simulated with different methods. These methods have usually been classified into two sections, global models and differential models, as in all methods the variable depends on crank angle (Stouffs et al., 2000). Using a global model, Stouffs et al. (Stouffs et al., 2000) investigated reciprocating compressors thermodynamically. In their model five main and four secondary parameters were important and obtained the volumetric effectiveness, the work per unit mass and the indicated efficiency. Casting et al. (Castaing-Lasvignottes and Gibout, 2010) modeled compressor operation using performance explanations like volumetric, isentropic and effective. They believed that these efficiencies depend fundamentally on two factors, the dead volumetric ratio which is of particular influence on volumetric efficiency, and a friction factor mainly influencing both on isentropic and effective efficiencies. Furthermore, Elhaj et al. (Elhaji et al., 2008) simulated a two-stage reciprocating compressor numerically. The main goal of their research was developing diagnostic features of predictive condition monitoring. Win and yet al. (Winandy et al., 2002) also proposed a simplified model of an open-type reciprocating compressor. Their analysis revealed the main processes affected by the refrigerant mass flow rate and the compressor power and the discharge temperature. Ndiaye et al. (Ndiaye and Bernier, 2010) presented a dynamic model of a hermetic reciprocating compressor in on-off cycling operation. Also Farzaneh-Gord et al. (Farzaneh-Gord et al., 2013) optimized design parameters of reciprocating air compressor thermodynamically. They developed a mathematical model according to the mass conservation and first law to study the performance of reciprocating compressors.

For a detailed examination of natural gas processes during pressure reduction, it is vital to calculate thermodynamic properties of natural gas mixture. One of the most accurate methods for computing these properties is the AGA8 Equation of State (AGA8–DC92 EoS, 1992; ISO-12213-2, 1997). Various studies have been carried out to compute thermodynamics properties of natural gas with using AGA8 EOS. Maric (Mari'c et al., 2005) calculated some of the thermodynamic properties of natural gas mixtures with using AGA8 EOS. Also, Farzaneh-Gord et al. (Farzaneh-Gord and Rahbari, 2012; Farzaneh-Gord et al., June 2010) have employed AGA8 EOS to compute variety of natural gas thermodynamic properties for various gas compositions.

As discussed above, there is possibility of employing reciprocating expansion engine in TBSs for simultaneous power generation and pressure reduction. To investigate feasibility of its employment, it is instructive to simulate and then optimize its operation under real conditions. Optimizations of reciprocating expansion engines parameters leads to more efficient employment of the machines. By simulating these engines, it is possible to investigate the impacts of various parameters on their performance and to identify the optimum design parameters. The modeling and simulation could also allow us to diagnose possible defects which reduce expansion engines efficiency.

In this research, the main purpose is to simulate one-sided reciprocating expansion engine thermodynamically for possible employment in TBSs. The thermodynamic simulation is based on first law of thermodynamics, conservation of mass and considering natural gas mixture as a real gas mixture. The thermodynamic properties of natural gas have been calculated based on AGA8 EOS. The simulation could predict thermodynamic properties (e.g. in-cylinder pressure and temperature) at various crank angles. Also, the effects of the engine geometric characteristics, such as intake and exhaust port area and ports timing on the work output have been studied.

2. The Town Border Stations (TBS)

In cities and nearby main consumers, the natural gas pipeline pressure is about 1.7 MPa (approximately 250 Psi). This pressure must be reduced to a distribution level (0.4 MPa (approximately 60 Psi)) in TBS station. Right now, the pressure reduction is accomplished by throttling valve, whereas significant amount of pressure energy is wasted. The reciprocating expansion engine is an effective instrument that can recover this waste energy. A schematic diagram of an expansion engine installed in a TBS is shown in Fig. 1.

3. Natural gas mixture

The chemical composition of natural gas changes with its composition which depends on geographic situation, the type, depth, and location of the underground deposit. Natural gas is processed and transported before reaching its end users. Table 1 shows an experimental analysis of a typical natural gas composition which flows in Iran pipe lines according to the Khangiran refinery official website. In this research, the composition of natural gas is assumed as Khangiran composition.

4. Methodology

A schematic of one-sided reciprocating expansion engine with suction and discharge ports is shown in Fig. 2. At the beginning of the cycle, suction port starts to open and let the gas to flow in the cylinder. With increasing in-cylinder pressure to medium pressure, the piston pushed down and therefore the cylinder volume increased. In this stage the suction process pressure makes constant. By closing the suction port, expanding process starts and piston reaches to Bottom Dead Centre (BDC). Then, by decreasing pressure to distributing level, discharge port opens and gas pushes out by coming up of piston. Ports move with crank shaft force and open/close in certain degrees. It should be noted that the control volume is assumed as an open system and also no leakage occur in the engine. The numerical modeling of the engine is discussed in this section.

4.1. First law of thermodynamics

For developing a numerical simulation, the conservation of mass and first law of thermodynamics has been employed. It should be noted that the inside cylinder gas is considered as control volume. The first law of thermodynamics is presented as follows:

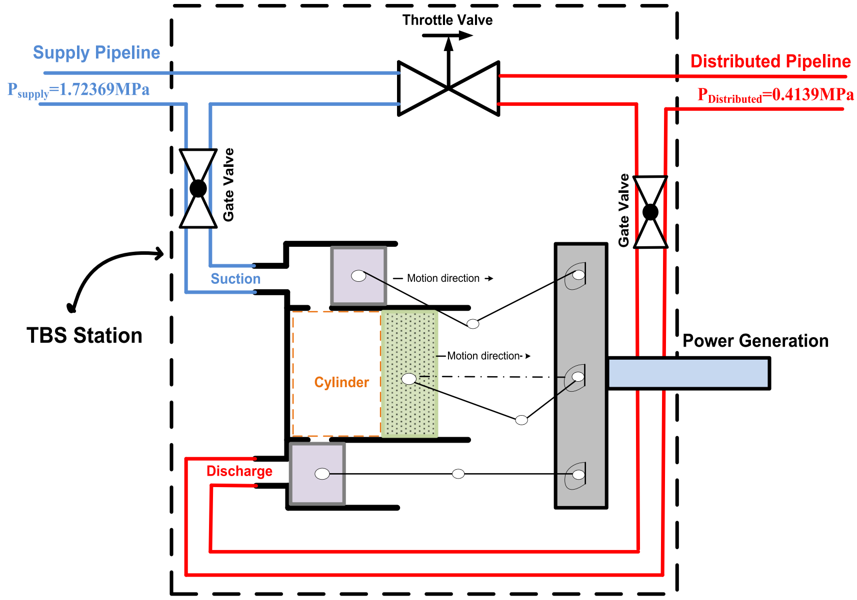

Fig. 1. Schematic diagram of natural gas TBS pressure drop station.

Table 1
Experimental analysis of natural gas composition the Khangiran refinery (the Khangiran refinery official website (Khangiran refinery official bsite)).

Component	Chemical formula	Experimental analysis (mole fraction %)
Carbon dioxide	CO_2	0.055
Nitrogen	N_2	0.428
Methane	CH_4	98.640
Ethane	C_2H_6	0.593
Propane	C_3H_8	0.065
Iso butane	C_4H_{10}	0.015
n-Butane	C_4H_{10}	0.034
Iso-Pentane	C_5H_{12}	0.026
$+C_6$	$+C_6$	0.125
		Total = 100%

$$\dot{Q}_{cv} + \sum \dot{m}_s\left(h_s + \frac{Ve_s^2}{2} + gH_s\right) = \sum \dot{m}_d\left(h_d + \frac{Ve_d^2}{2} + gH_d\right) + \frac{d}{dt}\left[m\left(u + \frac{Ve^2}{2} + gH\right)\right]_{cv} + \dot{W}_{cv} \quad (1)$$

If kinetic and potential energies are neglected, then the first law of thermodynamics could be changed as follow:

$$\frac{dQ_{cv}}{dt} + \frac{dm_s}{dt}h_s = \frac{dm_d}{dt}h_d + \frac{d}{dt}(mu)_{cv} + \frac{dW_{cv}}{dt} \quad (2)$$

The work changes can be computed as below:

$$\frac{dW_{cv}}{dt} = P_{cv}\frac{dV_{cv}}{dt} \quad (3)$$

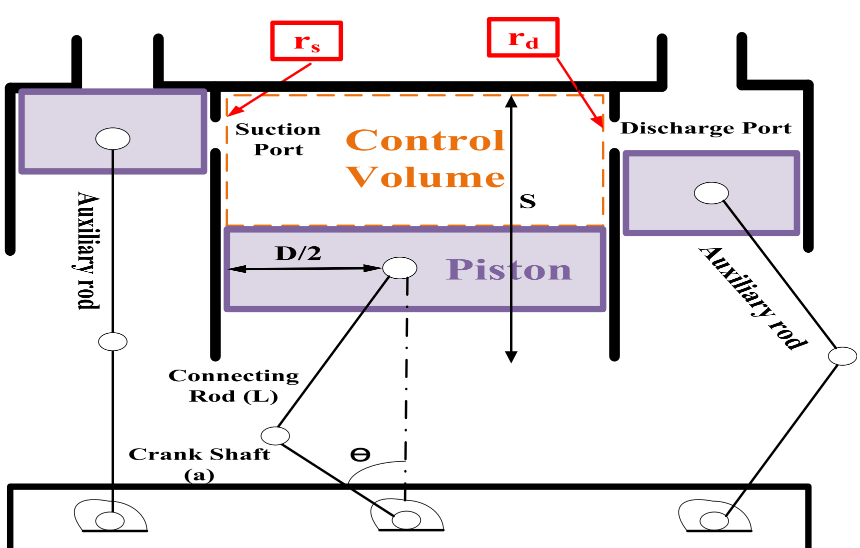

Fig. 2. A schematic diagram of a typical Reciprocating Expansion Engine.

By inserting equation (3) in equation (2), the next equation could be obtained:

$$\frac{dQ_{cv}}{dt}+\frac{dm_s}{dt}h_s=\frac{dm_s}{dt}h_s+\frac{d}{dt}(mu)_{cv}+\mathrm{P_{cv}}\frac{dV_{cv}}{dt} \tag{4}$$

Also, differentiating with respect to time could be converted to crank angle with by means of the following equation (Farzaneh-Gord and Rahbari, 2012):

$$\frac{d}{dt}=\frac{d}{d\theta}\times\frac{d\theta}{dt}=\omega\frac{d}{d\theta} \tag{5}$$

where ω is the rotational speed of the crank shaft. Eventually, the first law of thermodynamics equation appeared as below:

$$\frac{dQ_{cv}}{d\theta}+\frac{dm_d}{d\theta}h_d=\frac{dm_s}{d\theta}h_s+\frac{d}{d\theta}(mu)_{cv}+\mathrm{P_{cv}}\frac{dV_{cv}}{d\theta} \tag{6}$$

This equation is the main differential equation that will be solved as an initial condition ODE. In eq. (6) control volume is calculated with eq. (8), mass flow rates are calculated with the section 4.3 equations.

Thermodynamic properties will be also calculated with AGA8 model.

4.2. Piston motion equation

The detailed explanation for the immediate position of the piston displacement from top dead center in terms of the crank angle may be given by (Lee, 1983):

$$y(\theta)=\frac{S}{2}\left[1-\cos\theta+\frac{L}{a}\left(1-\sqrt{\left(1-(\frac{a}{L}\sin\theta)^2\right)}\right)\right] \tag{7}$$

where a, S and L are length of rod, stroke and crank respectively. The instantaneously volume of cylinder is given by:

$$V_{cv}=A_{cv}\times S(\theta)+V_0 \tag{8}$$

where V_0 is the dead volume.

4.3. Continuity equation

Considering the in-cylinder gas of expansion engine as a control volume, the continuity equation can be appeared as follows:

$$\frac{dm_{cv}}{d\theta}=\frac{dm_s}{d\theta}-\frac{dm_d}{d\theta} \tag{9}$$

where $dm_s/d\theta$ and $dm_d/d\theta$ are the mass flow rate through suction and discharge ports, respectively. By computing the flow velocity by Bernoulli equation without gravity terms, these mass flow rates could be computed through the following equations (Lee, 1983):

$$\dot{m}_s=\begin{cases}\rho_s A_s\sqrt{\dfrac{2(P_s-P_{cv})}{\rho_s}} & for \quad P_s>P_{cv}\\[2ex] \rho_{cv}A_s\sqrt{\dfrac{2(P_{cv}-P_s)}{\rho_{cv}}} & for \quad P_{cv}>P_s\end{cases} \tag{10}$$

$$\dot{m}_d=\begin{cases}\rho_{cv}A_d\sqrt{\dfrac{2(P_{cv}-P_d)}{\rho_s}} & for \quad P_{cv}>P_d\\[2ex] \rho_d A_d\sqrt{\dfrac{2(P_d-P_{cv})}{\rho_d}} & for \quad P_d>P_{cv}\end{cases} \tag{11}$$

where A_s and A_d are the flow areas through the suction and discharge ports which take place from cylinder, respectively. They are obtained by:

$$\begin{aligned}A_{smax}&=\pi r_s^2\\ A_{dmax}&=\pi r_d^2\end{aligned} \tag{12}$$

where r_s and r_d are radius of suction and discharge ports, respectively.

4.4. Ports movement equation

Suction and discharge ports are opened and close by auxiliary rods' motion. This motion is simulated as sinusoidal motion.

$$\mathrm{A}=\mathrm{A_{max}}\sin\left(\frac{\theta-\theta_{Open}}{\theta_{Close}-\theta_{Open}}\pi\right) \tag{13}$$

which A is efficient area during the opening/closing process, θ_{open} and θ_{close} are the crank shaft angles that the port opens or close and A_{max} is computed in eq. (12).

4.5. Heat transfer equation

Heat transfer due to overall heat transfer coefficient can be computed for each degree of crank angle from equation (14) as (Lee, 1983):

$$Q=UA_{(\theta)}\left(T_{(\theta)}-T_{am}\right) \tag{14}$$

where U,$A_{(\theta)}$,$T_{(\theta)}$ and T_{am} are the heat transfer coefficient, the heat transfer surface in each crank angle and in-cylinder gas temperature in each crank angle and the ambient temperature, respectively.

The overall heat transfer coefficient could be obtained as follow:

$$\mathrm{U}=\frac{1}{\mathrm{A_{Ref}}\sum\mathrm{Res}_j} \tag{15}$$

In which $\sum\mathrm{Res}_j$ is the total heat resistant of inside convection, wall conduction and outside convection that could be written as (Lee, 1983):

$$\sum\mathrm{Res}_j=\frac{1}{2\pi r_i y_{(\theta)}\alpha_i}+\frac{\log\frac{D_o}{D_i}}{2\pi\beta_i y_{(\theta)}}+\frac{1}{2\pi r_o y_{(\theta)}\alpha_o} \tag{16}$$

where the ambient heat coefficient could be computed as bellow (Lee, 1983):

$$Nu=\frac{\alpha D}{\beta}=\left(\frac{Gr\times\mathrm{Pr}_f^2}{2.435+4.884\sqrt{\mathrm{Pr}_f}+4.953\mathrm{Pr}_f}\right)^{0.25} \tag{17}$$

where Nu, α, D and β are Nusselt number, convection heat coefficient, cylinder outside diameter and conduction heat coefficient, respectively. $\mathrm{Pr}=C p\mu/K$ and f index is defined in film temperature:

$$T_f = \frac{T_w + T_{am}}{2} \tag{18}$$

The Grashof number is written as:

$$Gr = \frac{\left(\frac{\pi D}{2}\right)^3 g\left(\frac{T_{am}-T_w}{T_o}\right)}{\nu^2} \tag{19}$$

In which T_o is cylinder wall temperature. Also the wall conduction heat coefficient can be assumed as conduction heat coefficient of carbon steel in ambient temperature that is equal 50 W/(m K).

The Nusselt number of control volume is calculated by Hassan's equation (Lee, 1983):

$$Nu = \frac{\alpha_{in} D}{\beta} = 0.023\mathrm{Re}^{0.8} \tag{20}$$

here $\mathrm{Re} = C_m D/\nu$ is Reynolds number and $C_m = 2S\omega/60$ is mean piston speed with rotational speed of ω.

5. Computing thermodynamic properties of natural gas

It is evident that computing all in-cylinder properties needs two independent thermodynamic properties. Then other properties could be calculated according to these properties. The two properties are internal energy and density (or specific volume), which are calculated from first law of thermodynamics and conservation of mass, respectively. The methods of computing thermodynamic properties are summarized in this part. Details of the calculation of the thermodynamic properties can be seen in reference (Farzaneh-Gord and Rahbari, 2012).

5.1. AGA8 equation of state

The main relation of AGA8 equation of state can be written as follows (AGA8–DC92 EoS, 1992):

$$P = Z\rho_m RT \tag{21}$$

where Z and ρ_m are compressibility factor and molar density respectively. As it is clear, pressure and temperature is in Pascal and Kelvin units.

The Z factor could be computed by using the following equation [23]:

$$Z = 1 + B\rho_m - \rho_r \sum_{n=13}^{18} C_n^* + \sum_{n=13}^{18} C_n^* D_n^* \tag{22}$$

where Molar density, ρ_m, and reduced density, ρ_r, are interrelated as follows:

$$\rho_r = K^3 \rho_m \tag{23}$$

In equation (23), the K coefficient as the mixture size parameter is calculated as follows (AGA8–DC92 EoS, 1992):

$$K^5 = \left(\sum_{i=1}^{N} x_i K_i^{\frac{5}{2}}\right)^2 + 2\sum_{i=1}^{N-1}\sum_{j=i+1}^{N} x_i x_j \left(K_{ij}^5 - 1\right)\left(K_i K_j\right)^{\frac{5}{2}} \tag{24}$$

In above equation, x_i and x_j are mole fraction of component i and j in mixture respectively. Also, K_i and K_j are size parameters of component i and j respectively. Finally in equation (24), N is the number of components in the natural gas composition.

The method of calculating each of the coefficients in the equation (22) includes: B, C_n^* and D_n^* are presented in the references (AGA8–DC92 EoS, 1992; Farzaneh-Gord and Rahbari, 2012; Farzaneh-Gord et al., 2014, 2012).

By replacing equation (22) in equation (21), and with knowing the pressure (Pa), temperature (K) and natural gas composition, the only unknown property is molar density. For calculating the molar density is used of Newton–Raphson iterative method [23, 30, 31].

Finally the density could be obtained from:

$$\rho = M_w \rho_m \tag{25}$$

where M_w is molecular weight of natural gas mixture.

5.2. Computing enthalpy (h)

One of the thermal properties for natural gas is enthalpy. Supposing that enthalpy is a function of molar specific volume and temperature, the residual enthalpy equation can be expressed as (Moran and Shapiro, 2007):

$$h_m - h_{m,I} = \int_{\nu_{m,I}\to\infty}^{\nu_m} \left[T\left(\frac{\partial P}{\partial T}\right)_{\nu_m} - P\right] d\nu_m + \int_{\nu_{m,I}\to\infty}^{\nu_m} RT\left(\frac{\partial Z}{\partial \nu_m}\right)_T d\nu_m \tag{26}$$

In equation (26), h_m is molar enthalpy for real gas, $h_{m,I}$ molar enthalpy for ideal gas and $\nu_{m,I}$ is molar specific volume for ideal gas. By changing the variable of ν_m to ρ_m and calculating the partial differential values in equation (26), residual enthalpy function becomes as follows:

$$h_m - h_{m,I} = -RT^2 \int_0^{\rho_m} \left(\frac{\partial Z}{\partial T}\right)_{\rho_m} \frac{d\rho_m}{\rho_m} + RT(Z-1) \tag{27}$$

$h_{m,I}$ could be obtained by:

$$h_{m,I} = \sum_{j=1}^{N} x_j h_{m,i}^j \tag{28}$$

where x_j and $h_{m,i}^j$ are mole fraction of component j in mixture and molar enthalpy for ideal gas and for component j in mixture respectively.

$$h_{m,i}^j = h_{m,i0}^j + a_j T + b_j c_j \coth\left(\frac{c_j}{T}\right) - d_j e_j \tanh\left(\frac{e_j}{T}\right) \tag{29}$$

The parameter $h_{mi,o}^j$, in equation (29) is the enthalpy for ideal gas of component j in mixture at reference conditions. The method for calculating this parameter is described in reference (DIPPR® 801, 2004).

The partial differential relations in equation (26) have been calculated using AGA8 EOS. Finally by integrations from equation (27) and computing ideal molar enthalpy using equation (28), molar enthalpy is calculated for natural gas. The enthalpy per unit mass could be then calculated as follows:

$$h = \frac{h_m}{M_w} \tag{30}$$

5.3. Computing internal energy (u)

The relationship between the internal energy, u, and molar internal energy, u_m, can be defined as follows:

$$u = \frac{u_m}{M_w} \tag{31}$$

Also, the internal energy residual function could be computed as follow (Moran and Shapiro, 2007):

$$u_m - u_{m,I} = -RT^2 \int_0^{\rho_m} \left(\frac{\partial Z}{\partial T}\right)_{\rho_m} \frac{d\rho_m}{\rho_m} \tag{32}$$

In equation (32) $u_{m,I}$ is molar internal energy for ideal gas. This parameter can be computed by using the following formula:

$$u_{m,I} = h_{m,I} - P\nu_m = h_{m,I} - RT \tag{33}$$

6. Numerical procedure

As discussed above, to obtain two independent thermodynamic properties, first law and continuity equations which are presented at Eq. (6) and Eq. (9) are initially discretized as followed:

$$\frac{u_{n+1} - u_n}{\Delta\theta} = \frac{1}{m_{cv}} \left\{ \left(\frac{\Delta Q}{\Delta\theta}\right)_n + h_i \left(\frac{\Delta m_s}{\Delta\theta}\right)_n - P_{cv} \left(\frac{\Delta V}{\Delta\theta}\right)_n - h_d \left(\frac{\Delta m_d}{\Delta\theta}\right)_n - \omega \left(\frac{\Delta m_{cv}}{\Delta\theta}\right) u_n \right\} \tag{34}$$

$$\frac{\Delta m_{cv}}{\Delta\theta} = \frac{\dot{m}_s - \dot{m}_d}{\omega} \tag{35}$$

Then, the specific internal energy and m_{cv} are calculated from equations (34) and (35) for each crank angle by employing Runge–kotta method. Then density is calculated as below by knowing in–cylinder volume at each crank angle:

$$\rho_{(\theta)} = \frac{m_{cv(\theta)}}{V_{cv(\theta)}} \tag{36}$$

These two thermodynamic properties (density and specific internal energy) are enough to identify other thermodynamic parameters. For calculating pressure and temperature for each time step, thermodynamic table which has been formed by try and error method based on AGA8 EOS is used. The table is arranged according to internal energy (u) and density ($\rho_{(\theta)}$) (Table 2). Functions of pressure and temperature are prepared by Curve fitting method. These fittings are as 4th and 3rd degree for u and ρ respectively. Fig. 3 and Fig. 4 show the flowcharts of simulation code. Fig. 3 illustrates algorithm of pressure and temperature calculator. Fig. 4 shows the engine thermodynamic simulation which is employed in this study.

7. Results and discussion

The problem has been investigated for an expansion engine considering the specifications as following:

$$D_c = 15\text{ cm},\quad S = 12\text{ cm},\quad r_s = 2.5\text{ cm},\quad r_d = 3\text{ cm},\quad T_s = 280\text{ K}$$

Table 2
Pressure (MPa) arranged according to u and ρ.

ρ(kmol/m^3)	Um(kJ/kmol)				
	−1400	−990.8	−641.7	−300.1	500.2
0.1849	0.379	0.4	0.42	0.441	0.483
0.394	0.802	0.854	0.894	0.936	1.029
0.4639	0.943	1.003	1.052	1.101	1.21
0.6041	1.226	1.304	1.37	1.432	1.576
0.6978	1.413	1.503	1.581	1.654	1.82

The pressures of discharge plenum and pressure ratio are assumed to be 0.4 MPa and 4.25, respectively. The effects of different parameters of the problem on the results have been discussed separately.

The indicated work per in-cylinder mass is also calculated as below:

$$\mathrm{W_{indicated}} = \frac{1}{\mathrm{m_{cv}}} \int \mathrm{P dV} = \frac{1}{\mathrm{m_{cv}}} \sum_{i=1}^{N} \mathrm{P_i dV_i} \tag{37}$$

in which N is number of time steps and m_{cv} is the maximum in-cylinder mass value.

In this study, only the piston to cylinder wall friction (which is covered with a film of oil) has been considered.

Also the cylinder wall friction could be obtained as (Abu-Nada et al., 2008):

$$\delta W_{waste} = \mu \left(\frac{d\dot{y}}{d\varepsilon}\right)_{skirt} l_{skirt} \pi D \Delta y + \mu \left(\frac{d\dot{y}}{d\varepsilon}\right)_{ring} l_{ring} \pi D \Delta y \tag{38}$$

where l_{skirt}, l_{ring}, μ, Δy, ε and $\dot{y}$ are piston and piston ring lengths, oil viscosity, piston displacement, oil film thickness and piston speed.

So brake work could be calculated as:

$$\mathrm{W_{brake}} = \mathrm{W_{indicated}} - \int \delta \mathrm{W_{waste}} \tag{39}$$

Finally the efficiency of pressure energy recovery could be written as:

$$\eta = \frac{\mathrm{W_{brake}}}{\mathrm{h_o - h_{in}}} \tag{40}$$

In the first step, because of the lack of experimental values, for validation the numerical model in this study, the results of numerical method have been compared with theoretical results. For calculating the theoretical values, the thermodynamic conditions of expansion process are considered isentropic. Also the suction and discharge valves assumed to be closed. Based on this condition the values of in-cylinder pressure could be calculated as follows:

$$P_{cv}^{j+1} = P_{cv}^{j} \left(\frac{\nu_{cv}^{j+1}}{\nu_{cv}^{j}}\right)^k \tag{41}$$

Fig. 5 compares the variation of in-control volume pressure between numerical values and theoretical result against cylinder volume. As shown this figure, there is a good agreement between the theoretical and numerical values.

Fig. 6 shows the variation of in-cylinder pressures against cylinder volume for various angular speeds. In the numerical study, the suction and discharge pressures are assumed to be constant. In this Figure, as expected, suction and discharge processes are representative for constant-pressure evolution. Expansion happens as a polytrophic evolution and compression of residual mass is a constant-volume process.

Variation of in-cylinder temperatures against cylinder volume for one cycle and various angular speeds has been presented in Fig. 7. At the beginning suction process, temperature is increased by suddenly entering high temperature mass into the system. Then a decreasing trend starts till half of the cycle. Temperature dropping in suction process is mainly due to the specific volume decrement.

In expansion process, pressure and temperature drop occur simultaneously. In the discharge process, the pressure remains constant; therefore dropping density causes the temperature raising.

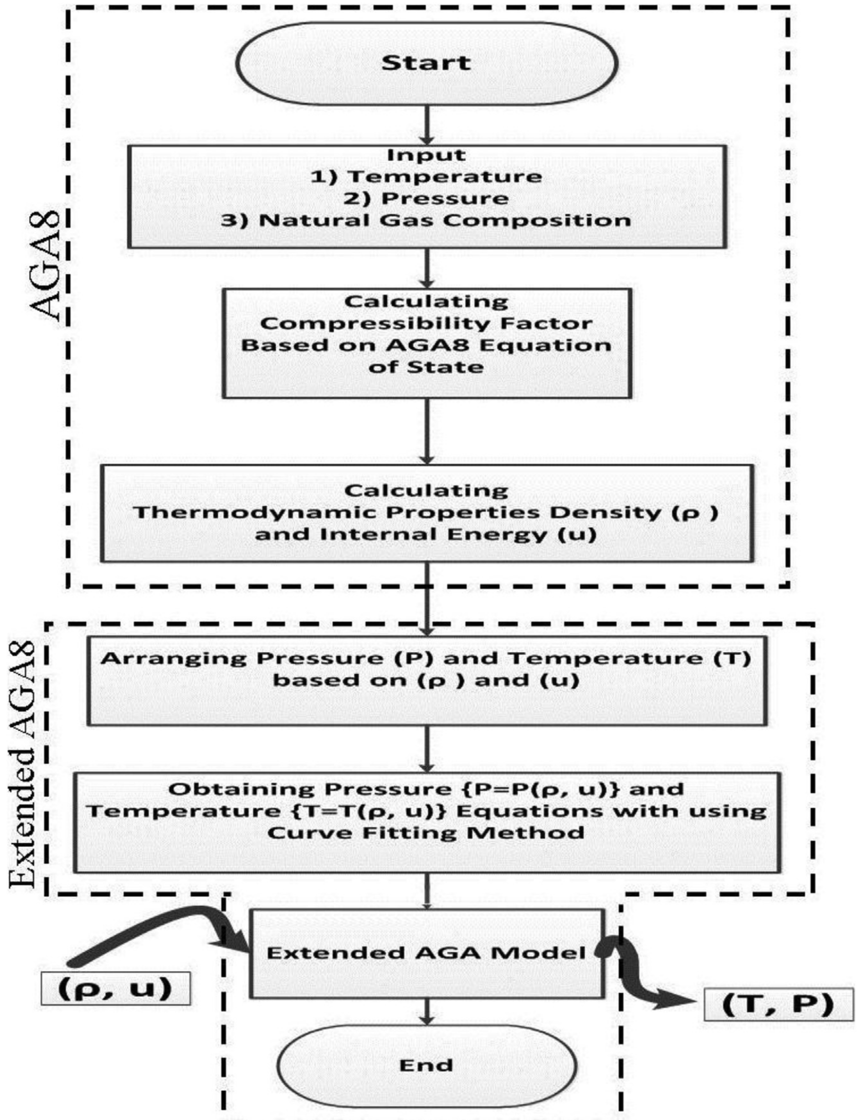

Fig. 3. Flowchart of extended AGA8 model.

The suction and discharge mass flow rates for various angular speeds are shown in Fig. 8. A suddenly mass entering occurs at the beginning of the suction. The reason is mainly due to the large difference between in-cylinder pressure and suction line pressure.

The variation of density is similar to pressure variation as shown in Fig. 9. Decreasing density at the second half of the cycle causes the temperature to rise.

Variation of in-cylinder mass as a function of crank shaft angle is shown in Fig. 10. The amount of gas in cylinder is raised while the suction port is open. Then this value remains constant during the expansion process. By opening the discharge port, a sudden discharge happens at the beginning but it continues with a more balanced procedure afterwards.

7.1. *Effect of port areas on engine performance*

The variation of output indicated work per cycle against different values of suction and discharge port is shown in Figure1 1. The port radius is assumed to be 2, 2.5, 3, 3.5 and 4 cm for suction and 2.5, 3, 3.5, 4 cm for discharge, respectively.

Fig. 11 illustrates that $r_S = 3$ cm for suction port is an optimized point.

Suction and discharge port diameters are one of the most important variables for motor optimizations. It could be declared, for certain, that increasing in-cylinder mass can cause an increment in the amount of output work. So investigations are done on variation of output work per mass of natural gas.

Variation of work per mass against radius of suction port is shown in Fig. 11. The figure is plotted at various values of discharge port radiuses. It shows that optimized diameter of suction port is $2r_S/D = 0.4$. The diameter of suction port affects to indicate work per cycle in two perspectives. With increasing suction port diameter, the greater amount of mass enters to cylinder and therefore more work is produced. In other hand, with increasing this diameter the pressure of the end of expansion will be different with discharge pressure and consequently the pressure exergy is wasted. Therefore for expansion engines could be selected optimized suction port diameter for obtaining maximum output work.

Fig. 11 also shows that increasing exhaust port radius increases the output work. So the best discharge port diameter is the

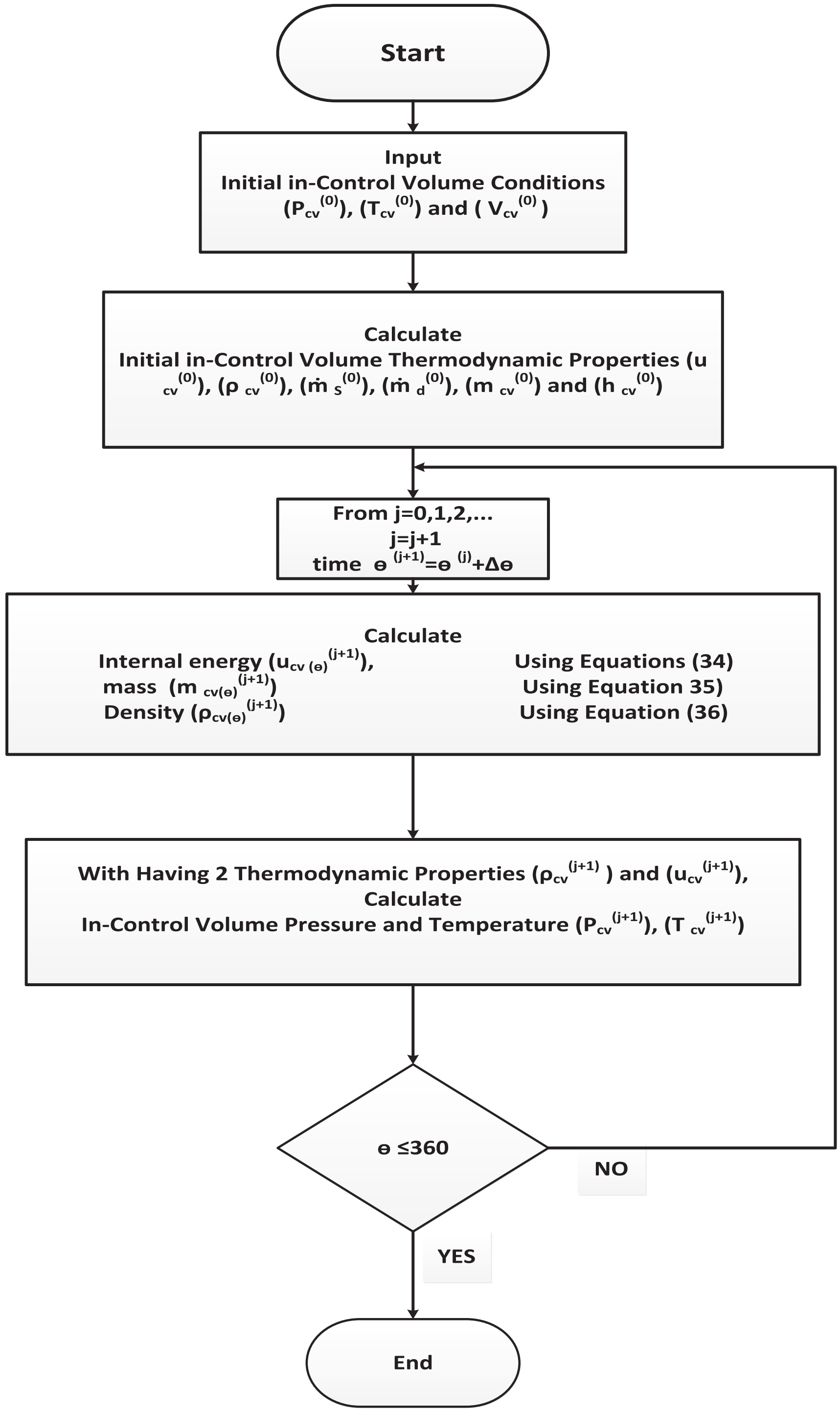

Fig. 4. Flowchart of simulation code.

maximum possible diameter. With increasing the discharge port diameter, the gas discharge at the back of piston is easier and consequently the in-cylinder pressure can be reduced. Therefore the discharge port diameter enhance the output indicate work per cycle and is dependent only on the engine size design.

7.2. Effect of port timing on engine performance

For investigation of port timing, it is assumed that suction port opens at the beginning of the cycle ($\theta = 0$) and discharge port closes at the end of the cycle. Accordingly, time of closure of suction port and opening of discharge port are studied.

According to port areas and motor geometry, the minimum adoptable value for suction port closure is 70° crank angle. Based on this, three values of 75, 85 and 95° for crank were tested for suction port closure. Discharge port opening is also considered in the range of 170–200 crank angles.

It could be concluded from Fig. 12 that the angle of 75° for suction port closure indicates the highest work per mass. Fig. 13 shows the effect of discharge port timing on output work. It

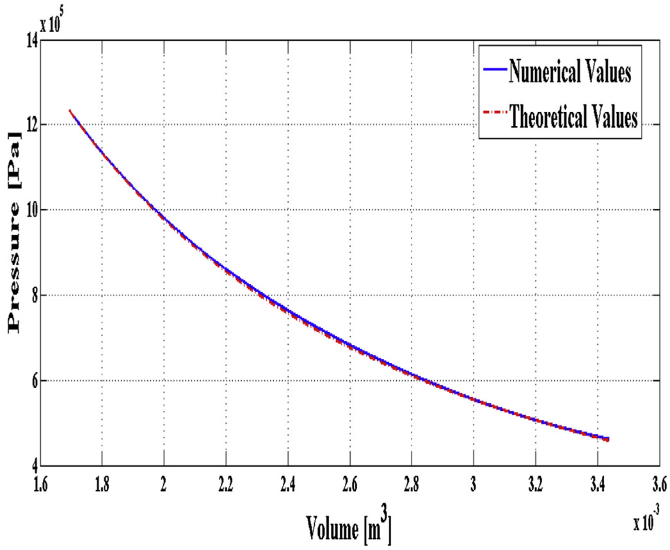

Fig. 5. Comparison between numerical and theoretical values of cylinder pressure.

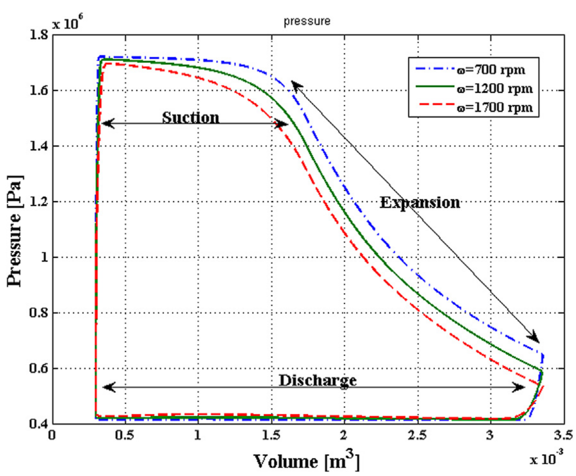

Fig. 6. Variation of in-cylinder pressures against volume for various angular speeds.

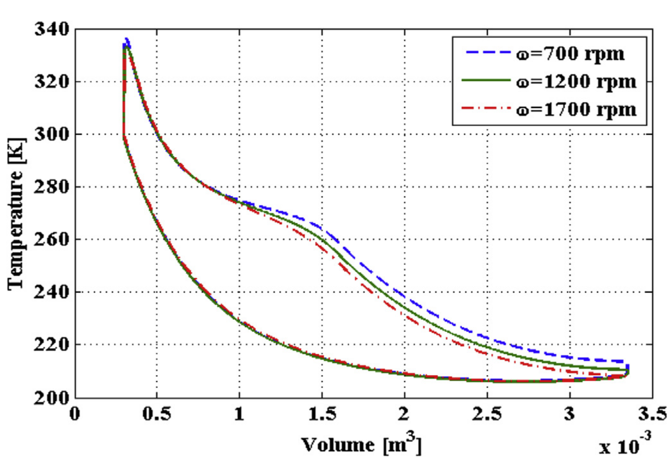

Fig. 7. Variation of in-cylinder temperatures vs. volume for various angular speeds.

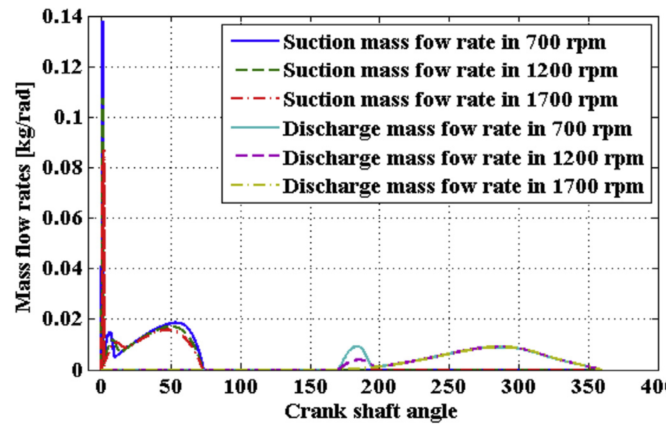

Fig. 8. Mass flow rate profiles vs. crank shaft angle for various angular speeds.

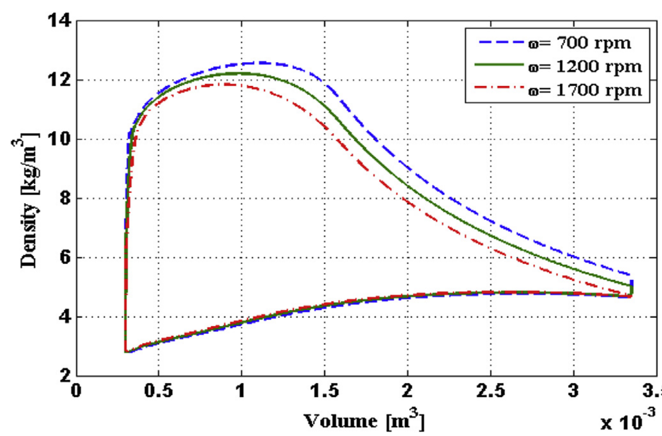

Fig. 9. in-cylinder density profiles vs. volume.

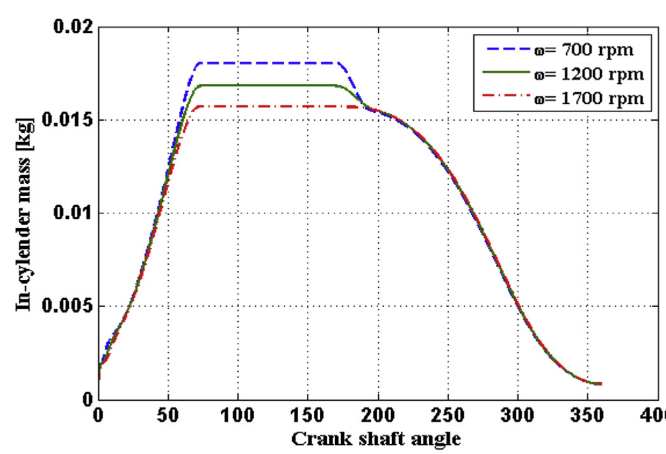

Fig. 10. Variation of in-cylinder masses vs. crank angle.

illustrates that the value of 182° for discharge port opening results in the most output work per mass.

In addition to the amount of indicated work, the mean exit gas temperature during discharge process has also been investigated. Based on the results from Fig. 14, delay in closing suction port and also delay in opening discharge port increase the outlet temperature.

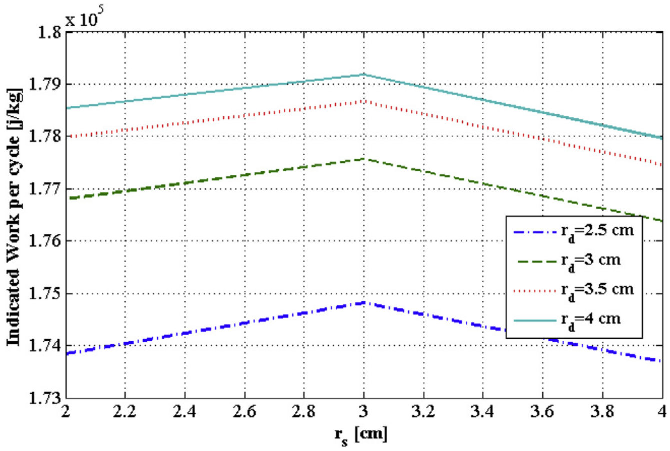

Fig. 11. Variation of indicated work per cycle vs. suction port radius in different discharge port radius.

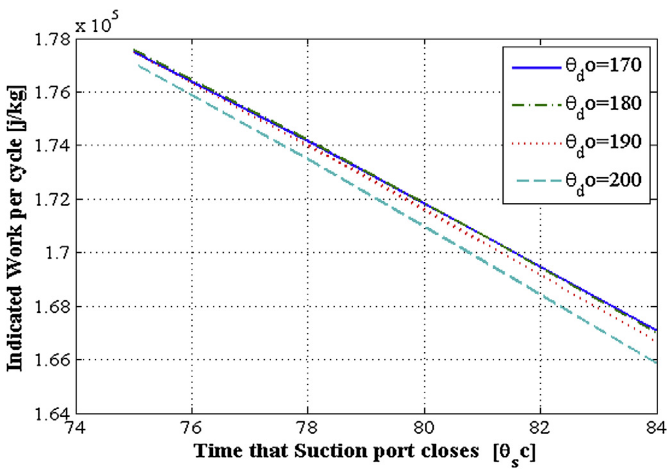

Fig. 12. Variation of output indicated work vs. suction duration.

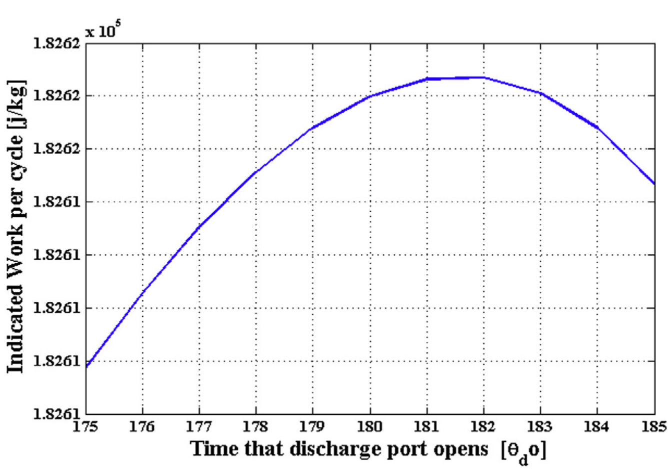

Fig. 13. Variation of output work vs. discharge duration.

7.3. Cost analysis

In this section the economic analysis for installing and setting up of expansion engine in TBS station is presented. According to calculations, the average power generation in TBS station with using expansion engine is about 46.2 kW. Therefore the net electricity generation is around 368.064MWh in 360 days of the year. It worth mentioning that 5 days per year is taken for maintenance periods. The benefit of this electricity generation is calculated to be 22083.84US$ based on the current electricity price in Iran which is 6 Cents/kWh.

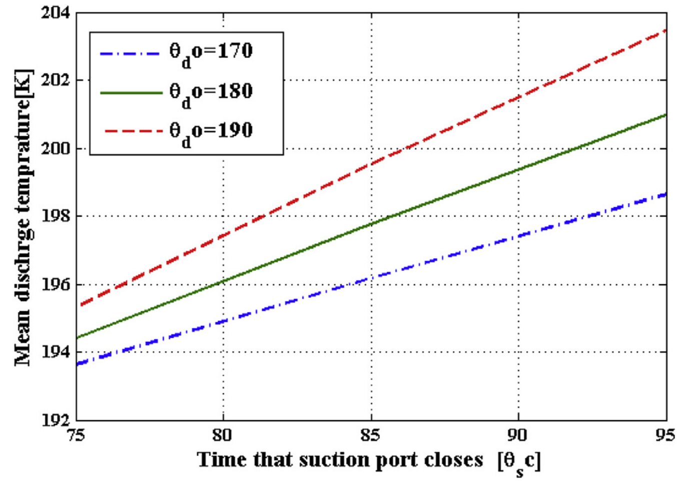

Fig. 14. Variation of discharge temperature vs. discharge duration.

Finally the payback ratio may be computed as follows:

$$Payback\ Ratio = \frac{(Capital + O\&M\ Costs)}{Benefit} = \frac{(30000 + 5000)}{22083.84} = 1.58$$

Table 3 presents the detailed cost analysis for the expansion engine system. Based on these results, the payback period has been calculated to be around 1.58 years. This revealed the cost effectiveness of the proposed system.

8. Conclusions

Reciprocating expansion engines could be used widely in gas pressure reduction stations due to their ability to recover considerable amount of energy. Understanding the behavior of the reciprocating expansion engines and studying the effects of various parameters on their performance can cause a needful optimization. The mathematical modeling is proved to be an effective tool to study performance of the expansion engines.

In this study, a mathematical model has been developed based on the first law of thermodynamics, conservation of mass, AGA8 EOS and thermodynamics relationships to study the performance of these engines. The model could predict in-cylinder pressure, in-cylinder temperature and mass flow rates at various crank angles. The indicated work per unit mass of gas is also calculated. The effects of various parameters on the performance of the expansion engine have been investigated as well.

The results show that ports timing is optimized at 75 degrees of crank angle for closing suction port and 182 degrees of crank angle for opening discharge port.

Table 3
The cost analysis of the expansion engine system.

Total capital cost for expansion engine installation	30000US$
Annual O&M costs	5000US$
Cost of electricity per kWh	0.06US$
Annual power generation	368.064MWh
Annual benefit	22083.84US$
Payback period	1.58year

Variation of indicator work verses ratio of discharge to suction ports shows that there is a specific value (about 0.85) in which the indicated work per unit mass is maximized. This point could be treated as optimum design value for discharge to suction port area.

Acknowledgment

Authors would like to thank the officials in Khorasan Razavi Gas Company for financial support.

References

Abu-Nada, E., Al-Hinti, I., Al-Sarkhi, A., Akash, B., 2008. Effect of piston friction on the performance of SI engine: a new thermodynamic approach. J. Eng. Gas Turbines Power 130 (MARCH).

AGA8–DC92 EoS, 1992. Compressibility and Super Compressibility for Natural Gas and Other Hydrocarbon Gases, Transmission Measurement Committee Report No. 8, AGA Catalog No. XQ 1285, Arlington, VA.

Bisio, G., 1995. Thermodynamic analysis of the use of pressure exergy of natural gas. Energy 20 (No. 2), 161–167.

Castaing-Lasvignottes, J., Gibout, S., 2010. Dynamic simulation of reciprocating refrigeration compressors and experimental validation. Int. J. Refrig. 33, 381–389.

Chaczykowski, M., Osiadacz, A.J., Uilhoorn, F.E., 2011. Exergy-based analysis of gas transmission system with application to Yamal-Europe pipeline. Appl. Energy 88, 2219–2230.

DIPPR 801, 2004. Evaluated standard thermophysical property values, design institute for physical properties. Spons. by AIChE 110–125.

Elhaji, M., Gu, F., Ball, A.D., Albarbar, A., 2008. Numerical simulation and experimental study of a two-stage reciprocating compressor for condition monitoring. Mech. Syst. Signal Process. 22, 374–389.

Farzaneh Gord, M., Jannatabadi, M., 2014. Simulation of single acting natural gas reciprocating expansion engine based on ideal gas model. J. Nat. Gas Sci. Eng. 21, 669–679.

Farzaneh-Gord, M., Deymi-Dashtebayaz, M., 2008. Recoverable energy in natural gas pressure drop stations: a case study of the Khangiran gas refinery. Energy Explor. Exploitation 26, 71–82.

Farzaneh-Gord, M., Deymi-Dashtebayaz, M., Hashemi, Sh., 2009. Improving the efficiency of an industrial gas turbine by a novel inlet air cooling method. J. Energy Inst. 82 (3), 150–158.

Farzaneh-Gord, M., Kargaran, M., 2010. Recovering energy at entry of natural gas into customer premises by employing a counter-flow vortex tube. Oil Gas Sci. Technology-Revue de l'IFP 65 (6), 903–912.

Farzaneh-Gord, M., Maghrebi, M.J., 2009. Exergy of natural gas flow in Iran's natural gas fields. Int. J. Exergy 6 (No. 1), 131–142, 2009.

Farzaneh-Gord, M., Rahbari, H.R., 2012. Numerical procedures for natural gas accurate thermodynamics properties calculation. J. Eng. Thermophys. 20 (2) to be published in the.

Farzaneh-Gord, M., Sadi, M., 2008. Enhancing energy output in Iran's natural gas pressure drop stations by cogeneration. J. energy Inst. 81 (No 4), 191–196.

Farzaneh-Gord, M., Hashemi, S., Sadi, M., 2009. Energy destruction in Iran's natural gas pipe line network. Energy Explor. Exploit. 25 (6).

Farzaneh-Gord, M., Deymi-Dashtebayaz, M., Rahbari, H.R., 2012. Optimizing compressed natural Gas refulling stations reservoir pressure based on thermodynamic analysis. Int. J. Exergy 10, 299–320.

Farzaneh-Gord, M., Niazmand, A., Deymi-DashteBayaz, M., 2013. Optimizing reciprocating air compressor design parameters based on first law analysis. U.P.B. Sci. Bull. Ser. D. 75 (4).

Farzaneh-Gord, M., Rahbari, H.R., Deymi-Dashtebayaz, M., 2014. Effects of natural gas compositions on CNG rapid refuelling process for buffer storage system. Oil Gas. Sci. Technol. 69, 319–330.

Farzaneh-Gord, M., Khamforoush, A., Hashemi, Sh, Pourkhadem, Namin H., June 2010. Computing thermal properties of natural gas by utilizing AGA8 equation of State. Int. J. Chem. Eng. Appl. 1 (No. 1).

Greeff, I.L., Visser, J.A., Ptasinski, K.J., Janssen, F.J.J.G., 2004. Using turbine expanders to recover exothermic reaction heat-flow sheet development for typical chemical processes. Energy 29, 2045–2060.

He, T.B., Ju, Y.L., 2014. A novel process for small-scale pipeline natural gas liquefaction. Appl. Energy 115, 17–24.

ISO-12213-2, 1997. Natural Gas- Calculation of Compression Factor-Part 2: Calculation Using Molar-composition Analysis, ISO, Ref. No. ISO- 12213-2:1997(E).

Khangiran refinery official website, http://khangiran.com/pages/Products.htm.

Kostowski, W., Usón, S., 2013. Thermoeconomic assessment of a natural gas expansion system integrated with a co-generation unit. Appl. Energy 101, 58–66.

Kostowski, W., Usón, S., Stanek, W., Bargiel, P., 2014. Thermo ecological cost of electricity production in the natural gas pressure reduction process. Energy xxx 1–9.

Lee, S., 1983. First Law Analysis of Unsteady Processes with Application to a Charging Process and a Reciprocating Compressor. The Ohaio State University. A Thesis presented in Partial Fulfillment of the Requirements for Degree of master Science.

Marić, I., Galović, A., Šmuc, T., 2005. Calculation of natural gas isentropic exponent. Flow Meas. Instrum. 16 (1), 13–20.

Moran, M.J., Shapiro, H.N., 2007. Fundamentals of Engineering Thermodynamics, sixth ed. Wiley, ISBN 0471787353.

Ndiaye, D., Bernier, M., 2010. Dynamic model of a hermetic reciprocating compressor in on-off cycling operation (Abbreviation: compressor dynamic model). Appl. Therm. Eng. 30, 792–799.

Querol, E., Gonzalez-Regueral, B., Garcıá-Torrent, J., Ramos, A., 2011. Available power generation cycles to be coupled with the liquid natural gas (LNG) vaporization process in a Spanish LNG terminal. Appl. Energy 88, 2382–2390.

Rosen, M.A., Scott, D.S., 1998. Energy and exergy analyses of a production process for methanol from natural gas. Int. J. Hydrogen Energy 13 (10), 617–623.

Stouffs, P., Tazerout, M., Wauters, P., 2000. Thermodynamic analysis of reciprocating compressors. Int. J. Thermodyn. Sci. 40, 52–66.

Tuma, M., Sekavcnik, M., 1997. Power generation by natural gas expansion engines. Fuel Energy Abstr. 38, 177.

Winandy, E., Saavedra, O., Lebrun, J., 2002. Simplified modelling of an open-type reciprocating compressor. Int. J. Sci. 41, 183–192.

Nomenclature

A: area (m^2)
a: crank (m)
c_p,c_v: constant pressure & volume specific heats (kJ/kg K)
C_m: mean piston speed (m/s)
D: cylinder diameter (m)
g: gravitational acceleration (m/s^2)
Gr: Grashof number
h: specific enthalpy (kJ/kg)
$\dot{m}$: mass flow rate (kg/s)
m: mass quantity (kg)
M: molecular weight (kg/k mol)
N: number of time steps
Nu: Nusselt number
L: connecting rod length (m)
P: pressure (bar or Pa)
Pr: Prandtl number
r: radius of suction and discharge ports (m)
R: gas global constant (J/mol K)
Re: Reynolds number
Res: the coefficient of thermal resistance (m^2K/kW)
$\dot{Q}$: heat transfer rate (kW)
S: stroke (m)
T: temperature (K or °C)
u: internal energy (kJ/kg)
U: overall heat transfer coefficient (kW/m^2 K)
V: volume (m^3/kg)
Ve: velocity (m/s)
W: actual work (kJ/kg)
$\dot{W}$: actual work rate (kW or MW)
x: mole fraction of component
y: position of the piston displacement (m)
$\dot{y}$: Piston speed (m/s)
Z: compressibility factor
H: height (m)

Subscript

am: ambient condition
d: discharge condition
in: inlet
i: inside
I: ideal
c: cylinder
cv: control volume condition
m: molar
max: maximum
r: reduced
Ref: reference
Ring: piston ring
o: outside
s: suction condition
skirt: piston skirt
w: wall
0: dead conditions

Greek letters

α: convection heat transfer coefficient (kW/m^2 K)
β: conduction heat transfer coefficient (kW/m K)
ρ: density (kg/m^3)
Θ: crank shaft angle (rad)

Ω: rotating speed of crankshaft (rad/s)
ρ_m: molar density
ρ_r: reduce density
γ: gas gravity
μ: oil viscosity (Pa s)
η: efficiency
ε: oil film thickness
ν_m: molar specific volume